



## Where Is the Drug? Quantitative 3D Distribution Analyses of Confined Drug-Loaded Polymer Matrices

Mazzoni, Chiara; Tentor, Fabio; Antalaki, Anastasia; Jacobsen, Rasmus D.; Mortensen, Jacob; Slipets, Roman; Ilchenko, Oleksii; Keller, Stephan S.; Nielsen, L. Hagner; Boisen, Anja

*Published in:*  
A C S Biomaterials Science & Engineering

*Link to article, DOI:*  
[10.1021/acsbiomaterials.9b00495](https://doi.org/10.1021/acsbiomaterials.9b00495)

*Publication date:*  
2019

*Document Version*  
Peer reviewed version

[Link back to DTU Orbit](#)

*Citation (APA):*  
Mazzoni, C., Tentor, F., Antalaki, A., Jacobsen, R. D., Mortensen, J., Slipets, R., Ilchenko, O., Keller, S. S., Nielsen, L. H., & Boisen, A. (2019). Where Is the Drug? Quantitative 3D Distribution Analyses of Confined Drug-Loaded Polymer Matrices. *A C S Biomaterials Science & Engineering*, 5(6), 2935-2941.  
<https://doi.org/10.1021/acsbiomaterials.9b00495>

---

### General rights

Copyright and moral rights for the publications made accessible in the public portal are retained by the authors and/or other copyright owners and it is a condition of accessing publications that users recognise and abide by the legal requirements associated with these rights.

- Users may download and print one copy of any publication from the public portal for the purpose of private study or research.
- You may not further distribute the material or use it for any profit-making activity or commercial gain
- You may freely distribute the URL identifying the publication in the public portal

If you believe that this document breaches copyright please contact us providing details, and we will remove access to the work immediately and investigate your claim.

## Controlled Release and Delivery Systems

**Where is the drug? - Quantitative 3D distribution analyses of confined drug-loaded polymer matrices**

Chiara Mazzoni, Fabio Tentor, Anastasia Antalaki, Rasmus Due Jacobsen, Jacob Mortensen, Roman Slipets, Oleksii Ilchenko, Stephan Sylvest Keller, Line Hagner Nielsen, and Anja Boisen

ACS Biomater. Sci. Eng., **Just Accepted Manuscript** • DOI: 10.1021/acsbmaterials.9b00495 • Publication Date (Web): 10 May 2019

Downloaded from <http://pubs.acs.org> on May 14, 2019

**Just Accepted**

“Just Accepted” manuscripts have been peer-reviewed and accepted for publication. They are posted online prior to technical editing, formatting for publication and author proofing. The American Chemical Society provides “Just Accepted” as a service to the research community to expedite the dissemination of scientific material as soon as possible after acceptance. “Just Accepted” manuscripts appear in full in PDF format accompanied by an HTML abstract. “Just Accepted” manuscripts have been fully peer reviewed, but should not be considered the official version of record. They are citable by the Digital Object Identifier (DOI®). “Just Accepted” is an optional service offered to authors. Therefore, the “Just Accepted” Web site may not include all articles that will be published in the journal. After a manuscript is technically edited and formatted, it will be removed from the “Just Accepted” Web site and published as an ASAP article. Note that technical editing may introduce minor changes to the manuscript text and/or graphics which could affect content, and all legal disclaimers and ethical guidelines that apply to the journal pertain. ACS cannot be held responsible for errors or consequences arising from the use of information contained in these “Just Accepted” manuscripts.

# Where is the drug? - Quantitative 3D distribution analyses of confined drug-loaded polymer matrices

*Chiara Mazzoni*<sup>\*\*</sup>, *Fabio Tentor*<sup>+</sup>, *Anastasia Antalaki*<sup>+</sup>, *Rasmus D. Jacobsen*<sup>+</sup>, *Jacob Mortensen*<sup>+</sup>, *Roman Slipets*<sup>+</sup>, *Oleksii Ilchenko*<sup>+</sup>, *Stephan S. Keller*<sup>◇</sup>, *L. Hagner Nielsen*<sup>+</sup>, *Anja Boisen*<sup>\*\*</sup>

<sup>+</sup> The Danish National Research Foundation and Villum Foundation's Center for Intelligent Drug Delivery and Sensing Using Microcontainers and Nanomechanics (IDUN) – Department of Health Technology, Technical University of Denmark, Ørsteds Plads Building 345C, Kgs. Lyngby, 2800, Denmark

<sup>◇</sup> The Danish National Research Foundation and Villum Foundation's Center for Intelligent Drug Delivery and Sensing Using Microcontainers and Nanomechanics (IDUN) –National Centre for Nano Fabrication and Characterization, Technical University of Denmark, Ørsteds Plads Building 345B, Kgs. Lyngby, 2800, Denmark

\* Corresponding authors: [chimaz@dtu.dk](mailto:chimaz@dtu.dk), [anja.boisen@dtu.dk](mailto:anja.boisen@dtu.dk)

## ABSTRACT

To enhance oral bioavailability of poorly soluble drugs, microfabricated devices can be utilized. One example of such devices is microcontainers. These are cylindrical in shape with an inner

1  
2  
3 cavity for drug loading and with only the top side open for release. Supercritical CO<sub>2</sub> (scCO<sub>2</sub>)  
4  
5 impregnation is an interesting technique for loading drugs into polymeric matrices in e.g.  
6  
7 microcontainers since it avoids the use of organic solvents and is cheap. One of the main  
8  
9 drawbacks of this technique is the unknown three dimensional drug distribution in the polymer  
10  
11 matrix. The aim of this study was to investigate the loading of two poorly soluble drugs,  
12  
13 naproxen and ketoprofen, by scCO<sub>2</sub> impregnation into confined polymer matrices of different  
14  
15 sizes. Three different sizes of microcontainers (small, medium and large) and thereby, different  
16  
17 surface areas accessible for impregnation, were compared. From *in vitro* studies, the amount of  
18  
19 naproxen and ketoprofen loaded into the different microcontainers and their corresponding  
20  
21 release profiles were seen to be similar. A custom-made Raman microscope facilitated  
22  
23 volumetric Raman maps of an entire microcontainer filled with polyvinylpyrrolidone (PVP) and  
24  
25 scCO<sub>2</sub> impregnated with either naproxen or ketoprofen. In all microcontainer sizes, the drugs  
26  
27 were only detected in the top layer of the polymer matrix, explaining the observed similar release  
28  
29 profiles. Using X-Ray Powder Diffraction and Raman spectroscopy, the solid state form of the  
30  
31 drugs was evaluated, showing that ketoprofen was amorphous in all microcontainer sizes.  
32  
33 Naproxen was found not to be crystalline neither amorphous, but in a less ordered configuration  
34  
35 than the crystalline state. In conclusion, volumetric Raman mapping is a powerful technology for  
36  
37 imaging drug distribution and drug crystallinity in polymers and allowed us to conclude that i)  
38  
39 scCO<sub>2</sub> impregnation depth does not depend on surface area and ii) impregnated drugs are non-  
40  
41 crystalline.  
42  
43  
44  
45  
46  
47  
48  
49

50  
51 KEYWORDS: Microdevices, polymer matrix, drug distribution, poorly soluble drug,  
52  
53 supercritical CO<sub>2</sub> impregnation, Raman spectroscopy  
54  
55  
56  
57  
58  
59  
60

## 1. INTRODUCTION

Among the different administration routes for drugs, oral delivery is preferred by patients since the drug can be self-administered leading to high compliance.<sup>1</sup> However, oral drug delivery is often challenging due to e.g. harsh conditions in the stomach and poor permeability over the intestinal wall.<sup>1</sup> Many drugs are classified as poorly water soluble in the biopharmaceutics classification system (BCS, class II and IV).<sup>2,3</sup> For oral delivery of poorly soluble drugs, solubility and dissolution rate need to be improved to obtain an acceptable bioavailability. One approach for achieving this, is to convert the drug to its amorphous form.<sup>4</sup> Here, the long range order in the crystal lattice is lacking and the disordered structure results in improved solubility and dissolution rate.<sup>4,5</sup> The disadvantage of the amorphous form is its physical and chemical instability. It can convert back to its metastable or stable counterpart during storage and/or dissolution.<sup>6</sup> There are various techniques to improve the physical stability of the amorphous form e.g. co-amorphization of two drugs<sup>7</sup> or use of polymers as excipients.<sup>8</sup> Another approach for protecting the amorphous drugs is the use of microcontainers.<sup>5,9</sup> Microcontainers are cylindrical, polymeric microdevices with an inner cavity for drug loading and with only the top side open. Previously, confinement of the amorphous poorly soluble drug indomethacin reduced the re-crystallization rate by 1.8 fold compared to unconfined bulk samples.<sup>5</sup> In particular, using microcontainers with cavity diameters of 174  $\mu\text{m}$ ,  $29.0 \pm 2.6$  % of the amorphous indomethacin crystallized over a period of 30 days compared to microcontainers with diameters of 223  $\mu\text{m}$  where  $38.3 \pm 1.5$  % crystallized. This indicates that microcontainers with smaller diameters enhance the stability of the amorphous drug loaded inside.<sup>5</sup> Unconfined indomethacin crystallized within a few days. In addition to the stabilization properties, microcontainers have been used for improving oral drug delivery by protecting the drug from the harsh gastric

1  
2  
3 environment and providing a release in the small intestine.<sup>10–12</sup> Furthermore, it has been  
4 demonstrated that microcontainers adhere to the intestinal mucus layer leading to higher relative  
5 oral bioavailability in rats of model drugs such as ketoprofen and furosemide compared to  
6 controls.<sup>13,14</sup>  
7  
8  
9  
10

11  
12 In spite of the advantages of utilizing microdevices for oral drug delivery, loading drugs into  
13 the small cavities can be challenging since all of the well-known techniques for preparing oral  
14 formulations, such as tableting, cannot be used. Supercritical CO<sub>2</sub> (scCO<sub>2</sub>) impregnation is one  
15 of the techniques that can be used for loading drugs into polymer-filled microcontainers. The  
16 critical point of CO<sub>2</sub> is 31.1°C and 73.8 bar and due to those mild conditions, this technique is  
17 suitable for drug loading. In addition, it can be used in combination with various polymers.<sup>15,16</sup> It  
18 has previously been demonstrated that the hydrophilic polymer polyvinylpyrrolidone (PVP) can  
19 be loaded into microcontainers as a polymer matrix and impregnated by scCO<sub>2</sub> with the drug  
20 ketoprofen.<sup>17,18</sup> It was found that ketoprofen was in its amorphous form after impregnation in the  
21 PVP matrix inside the microcontainers.<sup>14</sup> However, the influence of the size of the confined  
22 polymer volumes loaded by supercritical impregnation has never been investigated. One of the  
23 main challenges for systematic studies of drug loading with this technique has been the unknown  
24 three-dimensional (3D) drug distribution in the polymer matrix after CO<sub>2</sub> impregnation.  
25 Therefore, it has not been possible to understand the influence of the parameters on the release  
26 profiles and the drug-polymer interactions.<sup>16,17,19</sup>  
27  
28  
29  
30  
31  
32  
33  
34  
35  
36  
37  
38  
39  
40  
41  
42  
43  
44  
45  
46

47 In literature, the distribution of impregnated or encapsulated material has been studied with  
48 various techniques. Polymeric membranes have been examined with energy dispersive X-ray  
49 analyses, obtaining a two-dimensional map,<sup>19</sup> and this technique has also been successfully used  
50 for 3D mapping of nanoparticles.<sup>20</sup> Dispersive X-ray Absorption Spectroscopy ( $\mu$ ED-XAS)  
51  
52  
53  
54  
55  
56  
57  
58  
59  
60

1  
2  
3 tomography has been utilized and was able to resolve both 2D and 3D spatial distribution of  
4 chemical species from different iron mineral standards.<sup>21</sup> Alternatively, Raman spectroscopy has  
5 been used to evaluate the distribution of a drug inside a 3D printed tablet.<sup>22</sup> Previously, a 2D  
6 map of a cross section of tablets using Raman spectroscopy has been obtained, understanding the  
7 distribution of three different components in an area of 4 x 4 mm.<sup>23</sup> Raman spectroscopy has  
8 successfully been used as a quantification technique in case of inkjet-printed pharmaceuticals  
9 requiring, however, the sectioning of the sample prior to analyses in order to measure a cross  
10 section. <sup>24</sup> Cross sectional mapping with Raman spectroscopy is a destructive method and in case  
11 of a confined polymer matrix (i.e. for microcontainers) this application is not possible.  
12 Furthermore, for investigations with Raman spectroscopy, the polymer and drug normally have a  
13 relatively low transparency under laser excitation. For reaching an acceptable Raman signal at  
14 the bottom of samples as deep as e.g. a microcontainer reservoir, a highly sensitive method for  
15 confocal Raman microscope has been developed.

16  
17  
18  
19  
20  
21  
22  
23  
24  
25  
26  
27  
28  
29  
30  
31  
32  
33 The aim of this study was to investigate the loading of two BCS class II drugs, naproxen and  
34 ketoprofen, using scCO<sub>2</sub> impregnation into confined polymer matrices of different sizes. For this  
35 purpose, three different sizes of microcontainers (small, medium and large) and thereby,  
36 different surface areas accessible for impregnation were compared. Furthermore, the quantity  
37 and solid state form of ketoprofen and naproxen loaded into the microcontainers were evaluated.  
38 Finally, the 3D distribution of the drugs in 225 μm deep polymer matrices was analyzed by  
39 confocal Raman microscopy.

## 40 41 42 43 44 45 46 47 48 49 2. EXPERIMENTAL SECTION

### 50 51 2.1. MATERIALS

52  
53  
54  
55  
56  
57  
58  
59  
60

1  
2  
3 Silicon (Si) wafers (4-in, b100N n-type) were provided by Okmetic (Vantaa, Finland). SU-8  
4 2075 and SU-8 developer were purchased from Microresist Technology GmbH (Berlin,  
5 Germany). Polyvinylpyrrolidone (PVP) (Molecular weight of 10,000 Da), ketoprofen powder  
6 ( $\geq 98\%$ , racemate) and phosphate buffer saline (PBS) were obtained from Sigma-Aldrich (St.  
7 Louis, MO, USA). Naproxen was purchased from Fagron (Newcastle upon Tyne, England).  
8 Deionized water (18.2 m $\Omega$ ) was acquired from Merck KGaA (Darmstadt, Germany).  
9

## 16 2.2. METHODS

### 17 2.2.1. FABRICATION OF MICROCONTAINERS

18  
19 Squared chips of microcontainers with dimensions of 12.8 x 12.8 mm<sup>2</sup> were fabricated on Si  
20 wafers in the epoxy-based photoresist SU-8 using a similar procedure as described previously.<sup>5</sup>  
21  
22 Three different sizes of microcontainers were produced having three different cavity diameters  
23 (small, medium and large) and the same cavity height. The number of microcontainers per chip  
24 for the three different sizes was chosen to keep the total polymer surface exposed to the scCO<sub>2</sub>  
25 per chip constant, and thereby also the total polymer volume constant. The dimensions of the  
26 microcontainers were measured using an Alpha-Step IQ Stylus Profilometer (KLA-Tencor  
27 Corporation, Milpitas, USA) and an optical microscope.  
28  
29  
30  
31  
32  
33  
34  
35  
36  
37  
38

### 39 2.2.2. LOADING OF NAPROXEN AND KETOPROFEN INTO MICROCONTAINERS 40 USING SUPERCRITICAL CO<sub>2</sub> IMPREGNATION 41 42

43  
44 The microcontainers on Si chips were manually filled with PVP powder. Excess powder in  
45 between the microcontainers was blown away using an air gun in a similar setup as described  
46 previously.<sup>14</sup> One chip of each size (small, medium and large) was placed within a supercritical  
47 CO<sub>2</sub> chamber, together with 4.8  $\pm$  0.1 mg (n=3) of ketoprofen powder or 6.0  $\pm$  0.03 mg (n=3) of  
48 naproxen. The impregnation with ketoprofen was conducted by bringing CO<sub>2</sub> to its supercritical  
49  
50  
51  
52  
53  
54  
55  
56  
57  
58  
59  
60



1  
2  
3 state at 120 bar and 45°C keeping it under stirring for 1 h. The impregnation with naproxen was  
4 performed bringing CO<sub>2</sub> to 100 bar and 40°C. These parameters were chosen to have a solubility  
5 in the supercritical CO<sub>2</sub> of 0.06 g/L for both drugs.<sup>25,26</sup> The pressurization and depressurization  
6 rates were 3.9 bar/min and 2.5 bar/min, respectively, for both drugs. The chips with  
7 microcontainers were weighed before and after filling with PVP to determine the amount of  
8 polymer loaded into the microcontainers. A tabletop Scanning Electron Microscope (SEM)  
9 TM3030Plus (Hitachi High-Technologies, Tokyo, Japan) was used to visualize the  
10 microcontainers after filling with PVP and after the impregnation process.  
11  
12  
13  
14  
15  
16  
17  
18  
19  
20

### 21 2.2.3. *IN VITRO* RELEASE OF KETOPROFEN OR NAPROXEN FROM 22 MICROCONTAINERS 23 24 25

26 For determining the release of ketoprofen or naproxen over time, a  $\mu$ -Diss profiler (pION INC,  
27 Woburn, MA), equipped with *in situ* UV probes with a path length of 10 mm for ketoprofen and  
28 5 mm for naproxen was used. The release studies were performed in PBS at pH 6.5 for 120 min.  
29 Standard curves of either ketoprofen or naproxen were obtained before each release experiment.  
30 In order to prepare the standard curves, aliquots of a stock solution of ketoprofen (5 mg/mL in  
31 ethanol) or naproxen (3 mg/mL in ethanol) were added to known volumes of PBS, and the  
32 absorbance was assessed in a wavelength range of 250-260 nm for ketoprofen and at a  
33 wavelength of 230 nm for naproxen.  
34  
35  
36  
37  
38  
39  
40  
41  
42  
43

44 For release experiments, the chips with drug-loaded microcontainers were attached to  
45 cylindrical magnets and placed inside glass vials. 10 mL of PBS buffer were added to the vials  
46 immediately before starting an experiment. All the release studies were run at 37°C stirring the  
47 chips at 100 rpm. The experiments were performed in triplicates for each drug and for each size  
48  
49  
50  
51  
52  
53  
54  
55  
56  
57  
58  
59  
60

1  
2  
3 of microcontainers, the data are presented as mean (normalized by the quantity of PVP filled)  $\pm$   
4  
5 SD.  
6

#### 7 8 2.2.4. THREE-DIMENSIONAL DISTRIBUTION OF DRUGS IN MICROCONTAINERS 9

10 Volumetric Raman microscopy was used to evaluate the distribution of ketoprofen or naproxen  
11 in the microcontainers. The microscope collected Raman spectra in the range of 350-2400  $\text{cm}^{-1}$   
12 with a spectral resolution of 2.5  $\text{cm}^{-1}$  under the excitation of a 785 nm laser. The laser power was  
13 35 mW, and the diffraction limited spot size was equal to 1.7  $\mu\text{m}$  with the use of a 100x/0.75 HD  
14 DIC Zeiss microscope objective. The chip of microcontainers was placed on the surface of a  
15 custom-made Peltier stage and kept at 8°C during Raman measurements. These Raman spectra  
16 were studied performing a non-negative least squares analysis to obtain quantitative chemical  
17 response, visualized as voxel based 3D images.<sup>27,28</sup>  
18  
19  
20  
21  
22  
23  
24  
25  
26  
27

#### 28 2.2.5. SOLID STATE ANALYSES OF THE DRUGS LOADED INTO 29 30 MICROCONTAINERS 31 32

33 X-Ray Powder Diffraction (XRPD) was used to determine the solid state form of ketoprofen or  
34 naproxen in the microcontainers. An X'Pert PRO X-ray diffractometer (PANalytical, Almelo,  
35 The Netherlands, MPD PW3040/60 XRD; Cu KR anode,  $\lambda = 1.541 \text{ \AA}$ , 45 kV, 40 mA) was  
36 utilized. A starting angle of 5° 2 $\theta$  and an end angle of 28° 2 $\theta$  were employed for the scans with a  
37 scan speed of 0.67335° 2 $\theta$ /min and a step size of 0.0262606° 2 $\theta$ . Data were collected  
38 using X'Pert Data Collector software (PANalytical B.V.). The diffractograms of naproxen or  
39 ketoprofen loaded in the microcontainers were compared to the pure crystalline drugs. In  
40 addition, Raman microscopy was used to investigate the solid state form of the drugs. The  
41 spectra measured from the naproxen or ketoprofen loaded into the microcontainers were  
42 collected as described in "Three-dimensional distribution of the drugs in microcontainers"  
43  
44  
45  
46  
47  
48  
49  
50  
51  
52  
53  
54  
55  
56  
57  
58  
59  
60

section. For the spectra of crystalline and amorphous ketoprofen, naproxen and PVP the laser power was 35 mW and the exposure time was 2 s. The amorphous ketoprofen was prepared by melting the crystalline ketoprofen powder at 98°C on a heating plate followed by immediate measurements of the sample.

## 2.2.6. STATISTICS

All data are expressed as mean  $\pm$  standard deviation (SD). Statistical analyses were carried out, where relevant, using Student t-tests (GraphPad Prism, La Jolla, CA, USA, version 7.04). P-values below 5 % ( $p < 0.05$ ) were considered statistically significant.

## 2.3. RESULTS AND DISCUSSION

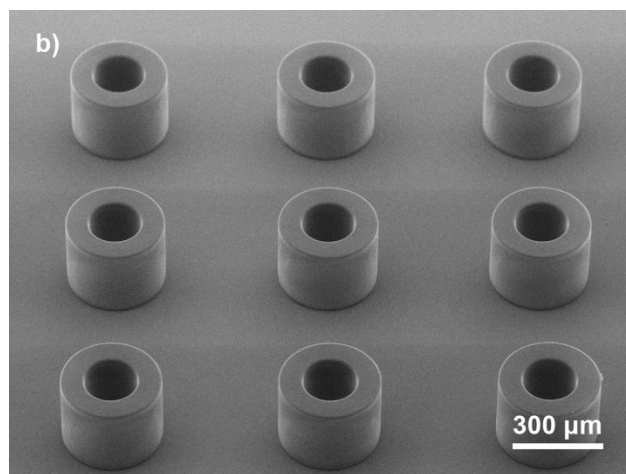
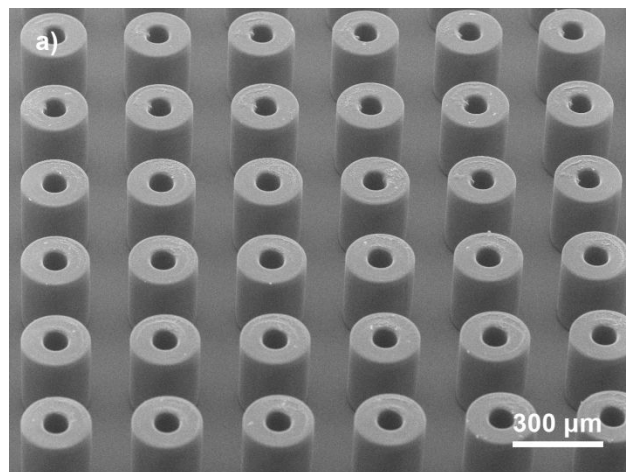
### 2.3.1. FABRICATION OF MICROCONTAINERS

Cylindrical microcontainers with three different sizes were successfully fabricated (Table 1 and Figure 1). The cavity depth of the microcontainers with the different sizes was kept constant at 225  $\mu\text{m}$ . The number of microcontainers per chip was chosen to keep the total polymer volume and the total surface area exposed to the supercritical  $\text{CO}_2$  similar for the different sizes (Table 1). Due to this, it was possible to compare the influence of the microcontainer size on quantity and distribution of the poorly soluble model drugs loaded with supercritical  $\text{CO}_2$  impregnation.

**Table 1.** Numbers showing the dimensions of the SU-8 microcontainers, amount of microcontainers per chip and total polymer surface area per chip. The data represents mean  $\pm$  SD in 8 replicates.

Sample	Internal microcontainer diameter [ $\mu\text{m}$ ]	Number of microcontainers per chip	Total polymer surface area exposed to $\text{scCO}_2$ per chip [ $\text{mm}^2$ ]

Small	$97 \pm 6$	1024	$31 \pm 4$
Medium	$191 \pm 9$	256	$30 \pm 3$
Large	$413 \pm 5$	64	$34 \pm 1$



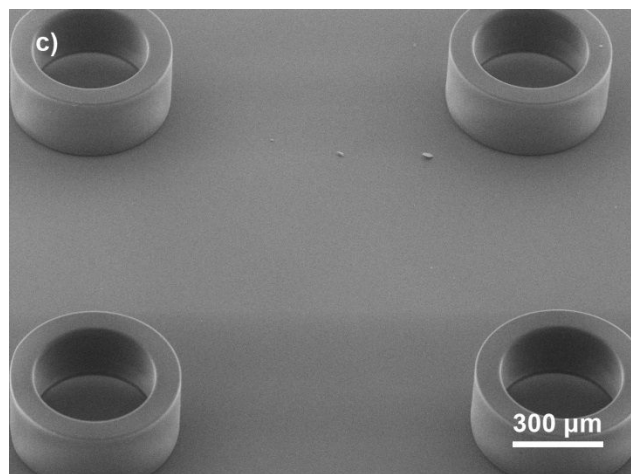


**Figure 1.** SEM images of SU-8 microcontainers in the size of a) small, b) medium and c) large having an internal diameter of  $97 \pm 6 \mu\text{m}$ ,  $191 \pm 9 \mu\text{m}$  and  $413 \pm 5 \mu\text{m}$ , respectively.

### 2.3.2. LOADING OF KETOPROFEN OR NAPROXEN INTO MICROCONTAINERS USING SUPERCRITICAL CO<sub>2</sub> IMPREGNATION

Every chip was manually filled with approximately 0.9 mg of PVP powder (Figure 2a), the amount varied slightly for the different sizes (Table 2). Followed by filling with PVP, one chip per size was then simultaneously loaded with ketoprofen or naproxen. An SEM image of the medium size microcontainers after scCO<sub>2</sub> impregnation with ketoprofen can be seen in Figure 2b. In a previous study, the amount of PVP filled per chip was higher.<sup>14</sup> This is due to the fact that, even if the medium size microcontainers have similar dimensions to that used in the previously reported study, the number of microcontainers is here reduced from 625 to 256.

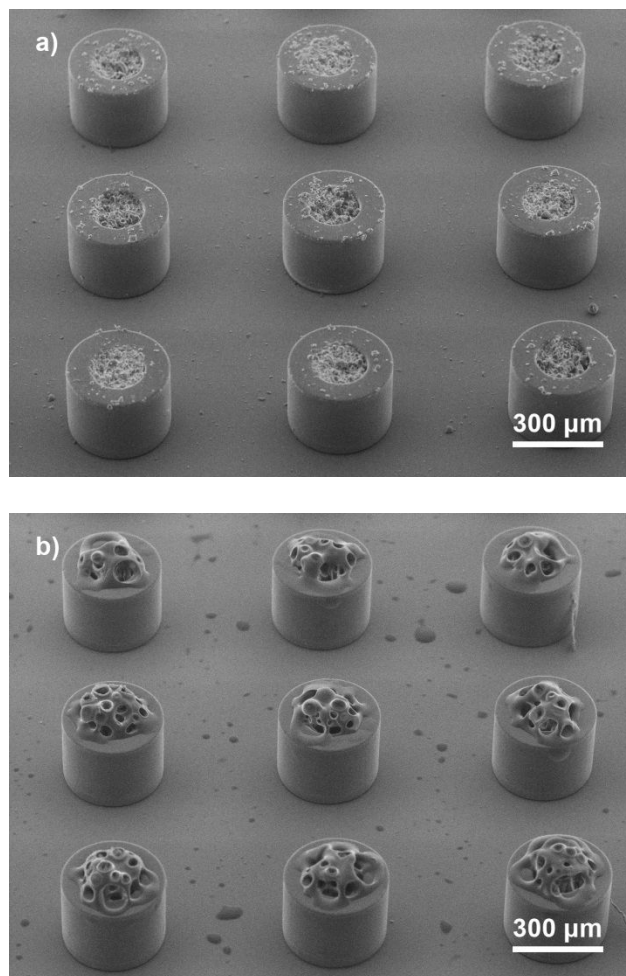


**Figure 2.** SEM images of medium sized microcontainers a) filled with PVP and b) loaded with ketoprofen using  $\text{scCO}_2$  impregnation. These images are representative examples of the PVP filling and the drug loading with the supercritical impregnation method.

### 2.3.3. *IN VITRO* RELEASE OF KETOPROFEN OR NAPROXEN FROM MICROCONTAINERS

The quantity of ketoprofen or naproxen loaded into the microcontainers with different sizes was evaluated in order to assess if there was an influence of the dimension of the surface exposed to  $\text{scCO}_2$ . The quantity of the loaded ketoprofen or naproxen in small, medium or large microcontainers was obtained from the release studies (Table 2 and Figure 3). The release profiles of the small, medium and large microcontainers loaded with ketoprofen showed similar

1  
2  
3 release profiles without any significant differences (Figure 3a). The same behavior was observed  
4  
5 in the case of naproxen (Figure 3b).  
6

7  
8 The total amount of ketoprofen loaded in the small size microcontainers compared to the  
9  
10 medium and large microcontainers was not significantly different (p-value: 0.4049 and p-value:  
11  
12 0.3667, respectively). No significant difference was observed between the loaded quantity of  
13  
14 ketoprofen in the medium and in the large microcontainers (p-value: 0.8098). The same  
15  
16 similarities, as observed for ketoprofen, were found for the total amount of loaded naproxen. In  
17  
18 fact, the amount of naproxen in the small size microcontainer was not statistically different to the  
19  
20 amount of drug in the medium or large microcontainers (p-value: 0.1071 and p-value: 0.2431,  
21  
22 respectively). Comparing the medium with the large size microcontainers, the total amount of  
23  
24 loaded naproxen also did not result in statistically different drug loadings (p-value = 0.3286).  
25  
26  
27  
28  
29

30  
31 Since the solubility of the two drugs in the scCO<sub>2</sub> was set to be the same, the release  
32  
33 experiments allowed for comparison of loading the two poorly water-soluble drugs into the  
34  
35 microcontainers with three different sizes. Within the first 10 min, 90 % of ketoprofen or  
36  
37 naproxen was released (Figure 3) from all sizes of microcontainers even if the release from small  
38  
39 microcontainers loaded with naproxen showed a larger variability. No statistical difference in the  
40  
41 loaded amount of ketoprofen or naproxen was discernible, independent of the size of the  
42  
43 microcontainers. Comparing the loaded amount of ketoprofen and naproxen in small  
44  
45 microcontainer sizes, the p-value was equal to 0.4374. For medium and large microcontainer  
46  
47 sizes, the p-values corresponded to 0.0642 and 0.1351, respectively.  
48  
49  
50

51  
52 Consequently, there was no difference in loading a BCS class II drug such as ketoprofen or  
53  
54 naproxen in a polymer matrix (PVP) having smaller or larger surfaces exposed to the scCO<sub>2</sub>.  
55  
56  
57  
58  
59  
60

1  
2  
3 This suggests that the size of the microcontainer opening has no influence on the quantity of drug  
4 loaded into the microcontainers. Furthermore, both BCS class II drugs were released with similar  
5 kinetics from the different sizes of microcontainers.  
6  
7  
8  
9

10 **Table 2.** Amount of ketoprofen or naproxen loaded in the three different sizes of  
11 microcontainers. The data represents mean  $\pm$  SD in triplicates.  
12  
13  
14

	Amount of PVP filled per chip [mg]	Total amount of ketoprofen loaded per chip [ $\mu$ g]	Total amount of naproxen loaded per chip [ $\mu$ g]
Small	0.94 $\pm$ 0.36	128.3 $\pm$ 65.9	89.7 $\pm$ 40.95
Medium	0.82 $\pm$ 0.1	91.3 $\pm$ 20.1	160.54 $\pm$ 42.8
Large	1.03 $\pm$ 0.17	86.1 $\pm$ 28.7	128.23 $\pm$ 26.50



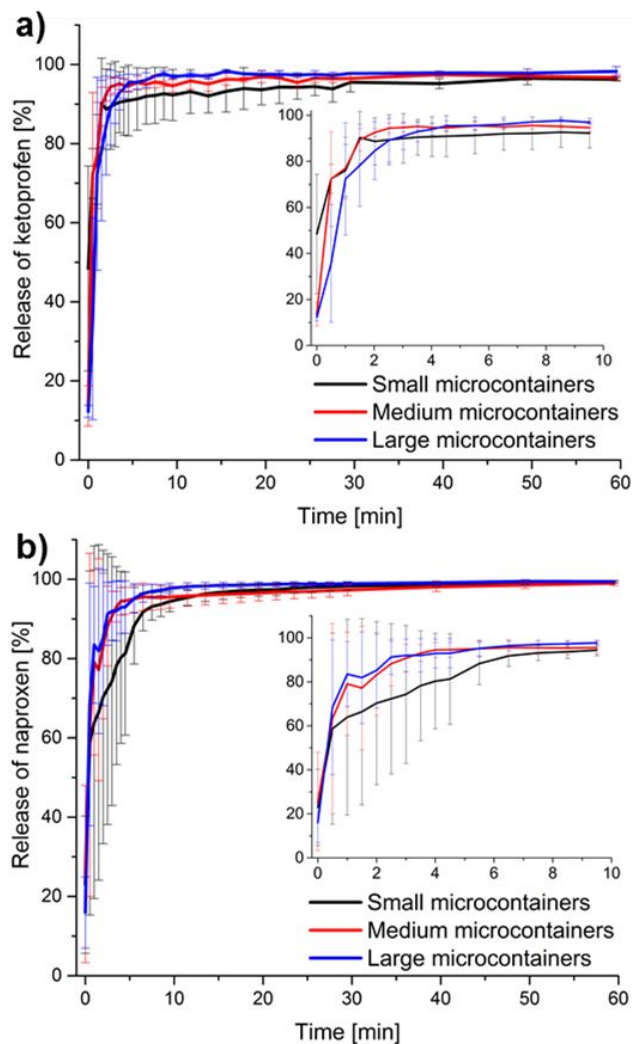


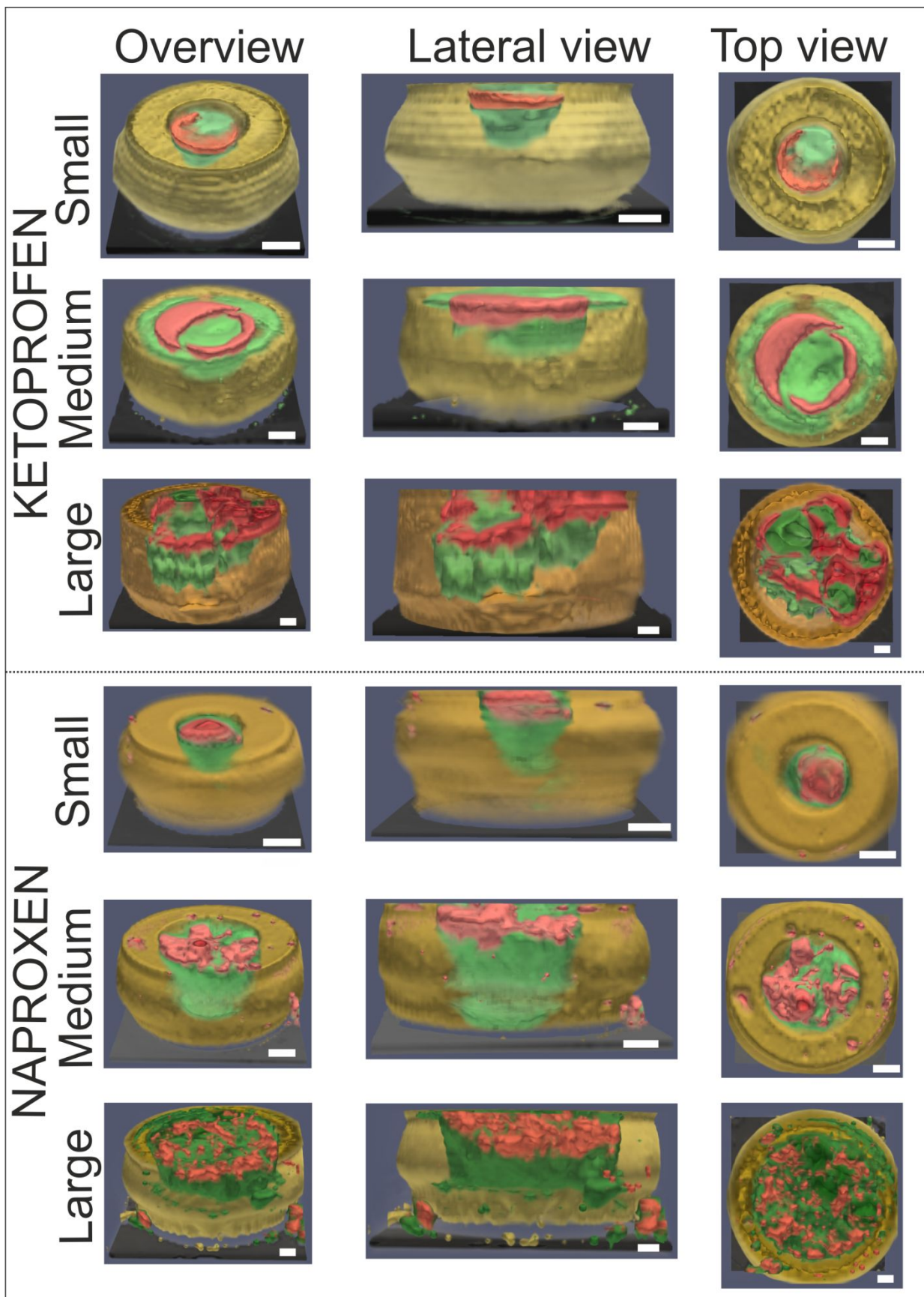
**Figure 3.** Release profiles of a) ketoprofen) and b) naproxen from small, medium and large microcontainers performed on a  $\mu$ -Diss profiler in PBS at pH 6.5. The inserts represent the same profiles zoomed in on the first 10 min. The graphs represent mean  $\pm$  SD in triplicates.

#### 2.3.4. THREE-DIMENSIONAL DISTRIBUTION OF DRUGS IN MICROCONTAINERS

It was possible to obtain 3D maps of polymer and drug-loaded microcontainers down to a depth of 225  $\mu$ m (the entire height of the microcontainer) using our custom-made Raman microscopy technique. To avoid heating of the sample, due to relatively high absorption of the laser, the temperature was kept constant at 8°C. To distinguish the various materials (PVP,

1  
2  
3 ketoprofen/naproxen, SU-8 or Si) in the samples, a chemical decomposition was performed on  
4 the spectra (Figure 4). In Figure 4, the same microcontainer 3D map reconstruction is shown in  
5  
6 three different perspectives: an overview, a cross section view and a top view.  
7  
8  
9

10 For all sizes of microcontainers loaded with either ketoprofen or naproxen, the drug was  
11 mainly impregnated in the top layers of the polymer matrix confined within the microcontainer  
12 walls. The results obtained in the *in vitro* release studies showed that both drugs reached 90 % of  
13 release within 10 min. The fast release could be explained by the fact that the drugs were mostly  
14 in the top part of the polymer matrix and not deep inside the microcontainer cavity. It is  
15 important to notice that the drug was distributed with the same morphology as PVP. It can  
16 therefore be speculated that, in a more porous polymer matrix, the drug could have penetrated  
17 deeper during the supercritical impregnation. In the top view of the microcontainers, it is  
18 possible to notice that both drugs were homogeneously distributed on the PVP. Furthermore,  
19 ketoprofen and naproxen were absent at the edge of the microcontainers meaning that both drugs  
20 were preferentially deposited in the PVP matrix and not in microcontainer material, SU-8. This  
21 technique can be useful to analyze polymer matrices for drug delivery in tissue engineering since  
22 the drug depth in the polymer matrix affects the release kinetic of the drug.<sup>29</sup> A pharmaceutical  
23 application, in which this technique can also be successfully used, is the characterization of tablet  
24 coatings as the presence of holes or different thicknesses can change the solubility kinetics of the  
25 tablet.<sup>30</sup>  
26  
27  
28  
29  
30  
31  
32  
33  
34  
35  
36  
37  
38  
39  
40  
41  
42  
43  
44  
45  
46  
47  
48  
49  
50  
51  
52  
53  
54  
55  
56  
57  
58  
59  
60



1  
2  
3 **Figure 4.** Volumetric Raman maps of ketoprofen or naproxen loaded into the microcontainers.  
4  
5 The overview, the lateral view and the top view can be seen from left to right for each of the  
6  
7 different sizes of microcontainers: small, medium and large from top to bottom. Ketoprofen or  
8  
9 naproxen are represented in red, PVP in green, SU-8 in yellow and Si in black. The scale bars  
10  
11 correspond to 50  $\mu\text{m}$ .  
12  
13  
14

### 15 2.3.5. SOLID STATE ANALYSES OF THE DRUGS LOADED INTO 16 17 MICROCONTAINERS 18 19

20 It has previously been shown that loading ketoprofen in a PVP matrix led to its conversion into  
21  
22 its amorphous form.<sup>14,18</sup> In Figure 5a, the diffractograms from XRPD of the small, medium and  
23  
24 large size of microcontainers loaded with ketoprofen showed a halo, distinctive of an amorphous  
25  
26 form. This indicated that the loaded ketoprofen was amorphous. In the case of naproxen loaded  
27  
28 into the PVP matrix in the different sizes of microcontainer, the diffractograms also showed a  
29  
30 halo for the small microcontainers (Figure 5b). For the medium and large microcontainers, the  
31  
32 halo still appeared, but with few peaks comparable to those of the crystalline diffractogram of  
33  
34 naproxen. Probably, a low crystallization of the drug occurred in the medium and large  
35  
36 microcontainers. In literature, studies have showed that when naproxen has been combined with  
37  
38 excipients or other drugs, a stable amorphous form could be obtained<sup>6,31</sup> despite the high  
39  
40 tendency of naproxen to recrystallize.<sup>32</sup> In particular, Liu et al. showed that naproxen was  
41  
42 amorphous even after 4 months when it was thermally treated and combined with PVP.<sup>6</sup> A  
43  
44 connection between the microcontainers size and the stability of the amorphous form of  
45  
46 naproxen may therefore exist. This confirms what has previously been shown: smaller sizes of  
47  
48 microcontainers prolong the stability of the amorphous form of indomethacin (BCS class II  
49  
50 drug).<sup>5</sup>  
51  
52  
53  
54  
55  
56  
57  
58  
59  
60

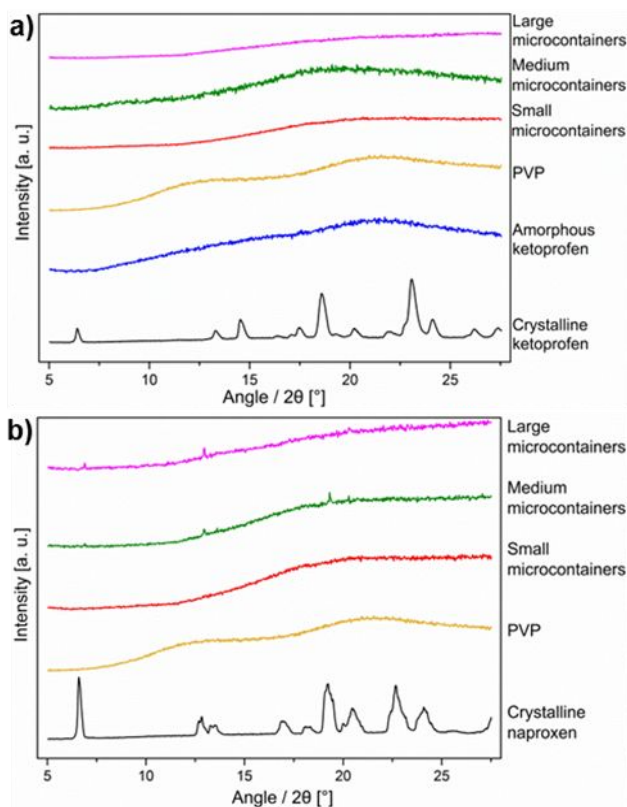
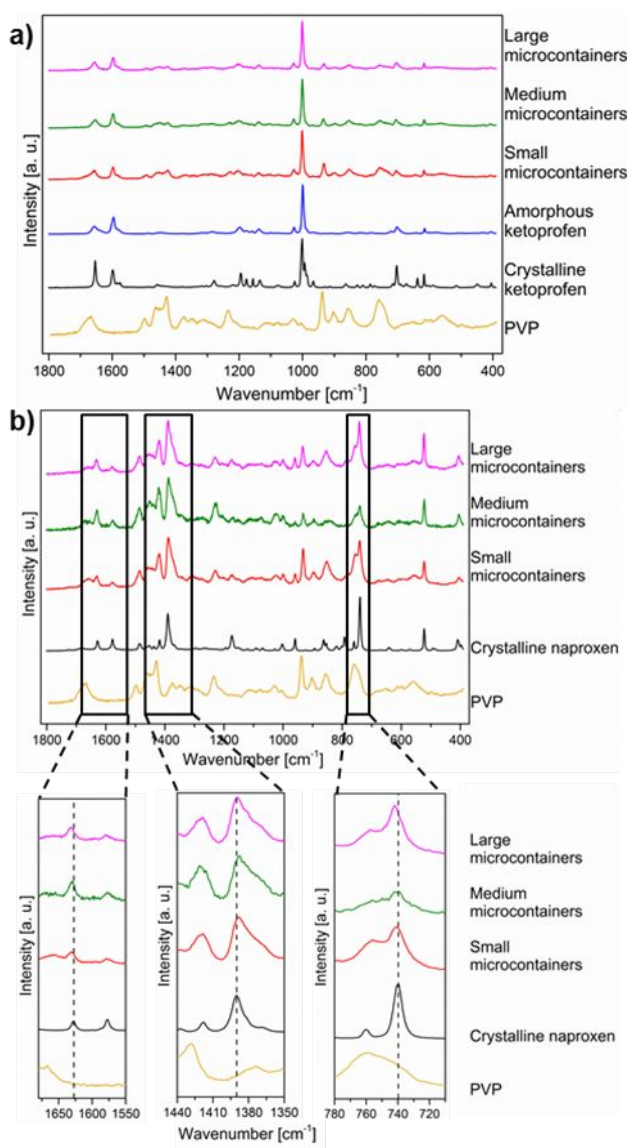


**Figure 5.** (a) XRPD diffractograms of crystalline and amorphous ketoprofen, PVP, small, medium and large microcontainers filled with PVP followed by impregnation with ketoprofen. (b) XRPD diffractograms of crystalline naproxen, PVP, small, medium and large microcontainers filled with PVP followed by impregnation with naproxen.

The results obtained by means of XRPD were confirmed by Raman spectroscopy for both drugs (Figure 6). The spectra from the microcontainers loaded with ketoprofen were similar to an amorphous ketoprofen spectrum, confirming that ketoprofen is amorphous when loaded in PVP matrices by  $\text{scCO}_2$  impregnation (Figure 6a).<sup>14</sup> Due to the instability of naproxen, it was not possible to obtain a Raman spectrum of its amorphous form. Therefore, the peak-shifts were analyzed (Figure 6b). In particular, the peaks at  $1626$ ,  $1390$  and  $740\text{ cm}^{-1}$  in the crystalline naproxen spectrum are shifted to  $1630$ - $1632$ ,  $1387$ - $1389$  and  $742\text{ cm}^{-1}$  in the spectra corresponding to microcontainers loaded with naproxen meaning that naproxen loaded in the

1  
2  
3 microcontainers is not in its crystalline form. The Raman signal from large microcontainers  
4 loaded with naproxen, at the wavenumber of  $740\text{ cm}^{-1}$ , showed a larger peak shift compared to  
5  
6  
7  
8 the other sizes of microcontainers (Figure 6b zoom-in). This might be due to the fact that the  
9  
10 Raman spectra were acquired from a random spot within a microcontainer in which also the  
11  
12 contribution from other materials might be measured. Previously, the same peak-shifts have  
13  
14 been considered, together with other techniques, to show the amorphous state of naproxen when  
15  
16 co-milled with cimetidine.<sup>33</sup>  
17  
18





1  
2  
3 **Figure 6.** a) Raman spectra of PVP, crystalline and amorphous ketoprofen, small, medium and  
4 large microcontainers filled with PVP followed by impregnation with ketoprofen. b) Raman  
5 spectra of PVP, crystalline naproxen, small, medium and large microcontainers filled with PVP  
6 followed by impregnation with naproxen. The zoom-in areas show the peak-shifts in naproxen  
7 loaded in microcontainers compared to its crystalline form.  
8  
9  
10  
11  
12  
13

## 14 15 CONCLUSIONS

16  
17 In this study, the influence of the surface exposed to scCO<sub>2</sub> was evaluated when loading two  
18 poorly water soluble drugs in a PVP polymer matrix confined in microcontainers. The release  
19 studies showed that the amount of loaded naproxen or ketoprofen was the same, when keeping  
20 the total surface area constant, and the release profiles were similar having 90 % of the drug  
21 released within 10 min. For microcontainers of different sizes, the loaded amount of drug nicely  
22 correlated with the surface area of the PVP matrix exposed to supercritical CO<sub>2</sub> during  
23 impregnation. To evaluate the 3D distribution of the drug in the polymer matrix in the  
24 microcontainers, a custom-made Raman microscope allowed obtaining volumetric Raman maps  
25 of the complete microcontainer volume. In the small, medium and large microcontainers,  
26 ketoprofen or naproxen were impregnated in the top of the polymer matrix explaining the fast  
27 release observed in the release studies. Moreover, the solid state form of the drugs was evaluated,  
28 showing that ketoprofen was amorphous in all microcontainers sizes and naproxen, despite its  
29 instability, was found only to be partly crystalline.  
30  
31  
32  
33  
34  
35  
36  
37  
38  
39  
40  
41  
42  
43  
44  
45  
46

## 47 SUPPLEMENTARY INFORMATION

48  
49 In the supplementary information, SEM images of microcontainers are shown. In Figure S1,  
50 SEM images of small and large microcontainers filled with PVP are presented, and SEM images  
51  
52  
53  
54  
55  
56  
57  
58  
59  
60

1  
2  
3 of the different sizes of microcontainers loaded by scCO<sub>2</sub> impregnation with either ketoprofen or  
4 naproxen are represented in Figure S2 and S3, respectively.  
5  
6

## 7 8 ACKNOWLEDGMENTS 9

10  
11 The authors would like to acknowledge the Danish National Research Foundation (DNRF122)  
12 and Villum Fonden (Grant No. 9301) for Intelligent Drug Delivery and Sensing Using  
13 Microcontainers and Nanomechanics (IDUN). Nanna Bild, DTU Nanotech, is acknowledged for  
14 the drawings of the graphical abstract.  
15  
16  
17  
18  
19

## 20 21 REFERENCES 22

- 23  
24  
25 (1) Tibbitt, M. W.; Dahlman, J. E.; Langer, R. Emerging Frontiers in Drug Delivery. *J. Am.*  
26 *Chem. Soc.* **2016**, *138* (3), 704–717. <https://doi.org/10.1021/jacs.5b09974>.  
27  
28  
29  
30 (2) Amidon, G. L.; Lennernäs, H.; Shah, V. P.; Crison, J. R. A Theoretical Basis for a  
31 Biopharmaceutic Drug Classification: The Correlation of in Vitro Drug Product  
32 Dissolution and in Vivo Bioavailability. *Pharm. Res.* **1995**, *12* (3), 413–420.  
33 <https://doi.org/http://dx.doi.org/10.1023/A:1016212804288>.  
34  
35  
36  
37 (3) Davis, M.; Walker, G. Recent Strategies in Spray Drying for the Enhanced Bioavailability  
38 of Poorly Water-Soluble Drugs. *J. Control. Release* **2018**, *269*, 110–127.  
39 <https://doi.org/10.1016/J.JCONREL.2017.11.005>.  
40  
41  
42 (4) Grohgan, H.; Priemel, P. A.; Löbmann, K.; Nielsen, L. H.; Laitinen, R.; Müllertz, A.;  
43 Van den Mooter, G.; Rades, T. Refining Stability and Dissolution Rate of Amorphous  
44 Drug Formulations. *Expert Opin. Drug Deliv.* **2014**, *11* (6), 977–989.  
45 <https://doi.org/10.1517/17425247.2014.911728>.  
46  
47  
48  
49  
50  
51  
52  
53  
54  
55  
56  
57  
58  
59  
60



- 1  
2  
3 (5) Nielsen, L. H.; Keller, S. S.; Gordon, K. C.; Boisen, A.; Rades, T.; Müllertz, A. Spatial  
4 Confinement Can Lead to Increased Stability of Amorphous Indomethacin. *Eur. J. Pharm.*  
5 *Biopharm.* **2012**, *81* (2), 418–425. <https://doi.org/10.1016/j.ejpb.2012.03.017>.  
6  
7  
8  
9  
10  
11 (6) Liu, X.; Zhou, L.; Zhang, F. Reactive Melt Extrusion To Improve the Dissolution  
12 Performance and Physical Stability of Naproxen Amorphous Solid Dispersions. *Mol.*  
13 *Pharm.* **2017**, *14* (3), 658–673. <https://doi.org/10.1021/acs.molpharmaceut.6b00960>.  
14  
15  
16  
17  
18 (7) Petry, I.; Löbmann, K.; Grohgan, H.; Rades, T.; Leopold, C. S. Undesired Co-  
19 Amorphisation of Indomethacin and Arginine during Combined Storage at High Humidity  
20 Conditions. *Int. J. Pharm.* **2018**, *544* (1), 172–180.  
21 <https://doi.org/10.1016/J.IJPHARM.2018.04.026>.  
22  
23  
24  
25  
26  
27  
28 (8) Ting, J. M.; Porter, W. W.; Mecca, J. M.; Bates, F. S.; Reineke, T. M. Advances in  
29 Polymer Design for Enhancing Oral Drug Solubility and Delivery. *Bioconjug. Chem.*  
30 **2018**, *29* (4), 939–952. <https://doi.org/10.1021/acs.bioconjchem.7b00646>.  
31  
32  
33  
34  
35  
36 (9) Nielsen, L. H.; Keller, S. S.; Boisen, A.; Müllertz, A.; Rades, T. A Slow Cooling Rate of  
37 Indomethacin Melt Spatially Confined in Microcontainers Increases the Physical Stability  
38 of the Amorphous Drug without Influencing Its Biorelevant Dissolution Behaviour. *Drug*  
39 *Deliv. Transl. Res.* **2014**, *4* (3), 268–274. <https://doi.org/10.1007/s13346-013-0166-7>.  
40  
41  
42  
43  
44  
45  
46 (10) Fox, C. B.; Cao, Y.; Nemeth, C. L.; Chirra, H. D.; Chevalier, R. W.; Xu, A. M.; Melosh,  
47 N. A.; Desai, T. A. Fabrication of Sealed Nanostraw Microdevices for Oral Drug  
48 Delivery. *ACS Nano* **2016**, *10* (6), 5873–5881. <https://doi.org/10.1021/acs.nano.6b00809>.  
49  
50  
51  
52  
53  
54 (11) Fox, C. B.; Nemeth, C. L.; Chevalier, R. W.; Cantlon, J.; Bogdanoff, D. B.; Hsiao, J. C.;  
55  
56  
57  
58  
59  
60

- 1  
2  
3 Desai, T. A. Picoliter-Volume Inkjet Printing into Planar Microdevice Reservoirs for  
4 Low-Waste, High-Capacity Drug Loading. *Bioeng. Transl. Med.* **2017**, *2* (1), 9–16.  
5  
6 <https://doi.org/10.1002/btm2.10053>.  
7  
8  
9  
10  
11 (12) Nielsen, L. H.; Nagstrup, J.; Gordon, S.; Keller, S. S.; Østergaard, J.; Rades, T.; Müllertz,  
12 A.; Boisen, A. PH-Triggered Drug Release from Biodegradable Microwells for Oral Drug  
13 Delivery. *Biomed. Microdevices* **2015**, *17* (3), 1–7. <https://doi.org/10.1007/s10544-015->  
14 [9958-5](https://doi.org/10.1007/s10544-015-9958-5).  
15  
16  
17  
18  
19  
20  
21 (13) Nielsen, L. H.; Melero, A.; Keller, S. S.; Jacobsen, J.; Garrigues, T.; Rades, T.; Müllertz,  
22 A.; Boisen, A. Polymeric Microcontainers Improve Oral Bioavailability of Furosemide.  
23 *Int. J. Pharm.* **2016**, *504* (1–2), 98–109. <https://doi.org/10.1016/J.IJPHARM.2016.03.050>.  
24  
25  
26  
27  
28  
29 (14) Mazzoni, C.; Tentor, F.; Strindberg, S. A.; Nielsen, L. H.; Keller, S. S.; Alstrøm, T. S.;  
30 Gundlach, C.; Müllertz, A.; Marizza, P.; Boisen, A. From Concept to in Vivo Testing:  
31 Microcontainers for Oral Drug Delivery. *J. Control. Release* **2017**, *268* (September), 343–  
32 351. <https://doi.org/10.1016/j.jconrel.2017.10.013>.  
33  
34  
35  
36  
37  
38  
39 (15) Kikic, I.; Vecchione, F. Supercritical Impregnation of Polymers. *Curr. Opin. Solid State*  
40 *Mater. Sci.* **2003**, *7* (4–5), 399–405. <https://doi.org/10.1016/J.COSSMS.2003.09.001>.  
41  
42  
43  
44 (16) Champeau, M.; Thomassin, J.-M.; Tassaing, T.; Jérôme, C. Drug Loading of Polymer  
45 Implants by Supercritical CO<sub>2</sub> Assisted Impregnation: A Review. *J. Control. Release*  
46 **2015**, *209*, 248–259. <https://doi.org/10.1016/J.JCONREL.2015.05.002>.  
47  
48  
49  
50  
51  
52 (17) Marizza, P.; Pontoni, L.; Rindzevicius, T.; Alopaeus, J. F.; Su, K.; Zeitler, J. A.; Keller, S.  
53 S.; Kikic, I.; Moneghini, M.; De Zordi, N.; et al. Supercritical Impregnation of Polymer  
54  
55  
56  
57  
58  
59  
60

- 1  
2  
3 Matrices Spatially Confined in Microcontainers for Oral Drug Delivery: Effect of  
4 Temperature, Pressure and Time. *J. Supercrit. Fluids* **2016**, *107*, 145–152.  
5  
6 <https://doi.org/10.1016/j.supflu.2015.08.023>.  
7  
8  
9  
10  
11 (18) Marizza, P.; Keller, S. S.; Müllertz, A.; Boisen, A. Polymer-Filled Microcontainers for  
12 Oral Delivery Loaded Using Supercritical Impregnation. *J. Control. Release* **2014**, *173*, 1–  
13 9. <https://doi.org/10.1016/j.jconrel.2013.09.022>.  
14  
15  
16  
17  
18 (19) Cardea, S.; Scognamiglio, M.; Reverchon, E. Supercritical Fluid Assisted Process for the  
19 Generation of Cellulose Acetate Loaded Structures, Potentially Useful for Tissue  
20 Engineering Applications. *Mater. Sci. Eng. C* **2016**, *59*, 480–487.  
21  
22 <https://doi.org/10.1016/J.MSEC.2015.10.053>.  
23  
24  
25  
26  
27  
28 (20) Slater, T. J.; Lewis, E. A.; Haigh, S. J. Energy Dispersive X-Ray Tomography for 3D  
29 Elemental Mapping of Individual Nanoparticles. *J. Vis. Exp* **2016**, No. 113, 52815.  
30  
31 <https://doi.org/10.3791/52815>.  
32  
33  
34  
35  
36 (21) Sanchez, D. F.; Simionovici, A. S.; Lemelle, L.; Cuartero, V.; Mathon, O.; Pascarelli, S.;  
37 Bonnin, A.; Shapiro, R.; Konhauser, K.; Grolimund, D.; et al. 2D/3D Microanalysis by  
38 Energy Dispersive X-Ray Absorption Spectroscopy Tomography. *Sci. Rep.* **2017**, *7* (1),  
39 16453. <https://doi.org/10.1038/s41598-017-16345-x>.  
40  
41  
42  
43  
44  
45  
46 (22) Trenfield, S. J.; Goyanes, A.; Telford, R.; Wilsdon, D.; Rowland, M.; Gaisford, S.; Basit,  
47 A. W. 3D Printed Drug Products: Non-Destructive Dose Verification Using a Rapid Point-  
48 and-Shoot Approach. *Int. J. Pharm.* **2018**, *549* (1–2), 283–292.  
49  
50 <https://doi.org/10.1016/J.IJPHARM.2018.08.002>.  
51  
52  
53  
54  
55  
56  
57  
58  
59  
60

- 1  
2  
3 (23) Cerea, M.; Maroni, A.; Palugan, L.; Bellini, M.; Foppoli, A.; Melocchi, A.; Zema, L.;  
4  
5 Gazzaniga, A. Novel Hydrophilic Matrix System with Non-Uniform Drug Distribution for  
6  
7 Zero-Order Release Kinetics. *J. Control. Release* **2018**, *287*, 247–256.  
8  
9 <https://doi.org/10.1016/J.JCONREL.2018.08.027>.  
10  
11  
12  
13 (24) Edinger, M.; Bar-Shalom, D.; Rantanen, J.; Genina, N. Visualization and Non-Destructive  
14  
15 Quantification of Inkjet-Printed Pharmaceuticals on Different Substrates Using Raman  
16  
17 Spectroscopy and Raman Chemical Imaging. *Pharm. Res.* **2017**, *34* (5), 1023–1036.  
18  
19 <https://doi.org/10.1007/s11095-017-2126-2>.  
20  
21  
22  
23 (25) Ting, S. S. T.; Macnaughton, S. J.; Tomasko, D. L.; Foster, N. R. Solubility of Naproxen  
24  
25 in Supercritical Carbon-Dioxide with and without Cosolvents. *Ind. Eng. Chem. Res.* **1993**,  
26  
27 *32* (7), 1471–1481. <https://doi.org/10.1021/Ie00019a022>.  
28  
29  
30  
31 (26) Garmroodi, A.; Hassan, J.; Yamini, Y. Solubilities of the Drugs Benzocaine,  
32  
33 Metronidazole Benzoate, and Naproxen in Supercritical Carbon Dioxide. *J. Chem. Eng.*  
34  
35 *Data* **2004**, *49* (3), 709–712. <https://doi.org/10.1021/je020218w>.  
36  
37  
38  
39 (27) Ilchenko, O.; Pilgun, Y.; Makhnii, T.; Slipets, R.; Reynt, A.; Kutsyk, A.; Slobodianiuk,  
40  
41 D.; Koliada, A.; Krasnenkov, D.; Kukharsky, V. High-Speed Line-Focus Raman  
42  
43 Microscopy with Spectral Decomposition of Mouse Skin. *Vib. Spectrosc.* **2016**, *83*, 180–  
44  
45 190. <https://doi.org/10.1016/J.VIBSPEC.2016.02.003>.  
46  
47  
48  
49 (28) Ilchenko, O. O.; Pilgun, Y. V.; Reynt, A. S.; Kutsyk, A. M. NNLS and MCR-ALS  
50  
51 Decomposition of Raman and FTIR Spectra of Multicomponent Liquid Solutions. *Ukr. J.*  
52  
53 *Phys.* **2016**, *61* (6), 519–522. <https://doi.org/10.15407/ujpe61.06.0519>.  
54  
55  
56  
57  
58  
59  
60

- 1  
2  
3 (29) Gaikwad, V. V.; Patil, A. B.; Gaikwad, M. V. Scaffolds for Drug Delivery in Tissue  
4 Engineering. *Int. J. Pharm. Sci. Nanotechnol.* **2008**, *1* (2), 113–122.  
5  
6  
7  
8  
9 (30) El Hagrasy, A. S.; Chang, S.-Y.; Desai, D.; Kiang, S. Raman Spectroscopy for the  
10 Determination of Coating Uniformity of Tablets: Assessment of Product Quality and  
11 Coating Pan Mixing Efficiency during Scale-Up. *J. Pharm. Innov.* **2006**, *1* (1), 37–42.  
12  
13 <https://doi.org/10.1007/BF02784879>.  
14  
15  
16  
17  
18 (31) Beyer, A.; Grohganz, H.; Löbmann, K.; Rades, T.; Leopold, C. S. Influence of the  
19 Cooling Rate and the Blend Ratio on the Physical Stability of Co-Amorphous  
20 Naproxen/Indomethacin. *Eur. J. Pharm. Biopharm.* **2016**, *109*, 140–148.  
21  
22 <https://doi.org/10.1016/J.EJPB.2016.10.002>.  
23  
24  
25  
26  
27  
28 (32) Sibik, J.; Löbmann, K.; Rades, T.; Zeitler, J. A. Predicting Crystallization of Amorphous  
29 Drugs with Terahertz Spectroscopy. *Mol. Pharm.* **2015**, *12* (8), 3062–3068.  
30  
31 <https://doi.org/10.1021/acs.molpharmaceut.5b00330>.  
32  
33  
34  
35  
36 (33) Allesø, M.; Chieng, N.; Rehder, S.; Rantanen, J.; Rades, T.; Aaltonen, J. Enhanced  
37 Dissolution Rate and Synchronized Release of Drugs in Binary Systems through  
38 Formulation: Amorphous Naproxen–cimetidine Mixtures Prepared by Mechanical  
39 Activation. *J. Control. Release* **2009**, *136* (1), 45–53.  
40  
41 <https://doi.org/10.1016/J.JCONREL.2009.01.027>.  
42  
43  
44  
45  
46  
47  
48  
49  
50  
51  
52  
53  
54  
55  
56  
57  
58  
59  
60

1  
2  
3 “For table of Contents only”  
4  
5  
6  
7

8  
9 **Where is the drug? - Quantitative 3D distribution**  
10  
11  
12  
13 **analyses of confined drug-loaded polymer matrices**  
14  
15  
16  
17

18 *Chiara Mazzoni\**, *Fabio Tentor*, *Anastasia Antalaki*, *Rasmus D. Jacobsen*, *Jacob Mortensen*,  
19  
20  
21 *Roman Slipets*, *Oleksii Ilchenko*, *Stephan S. Keller*, *Line H. Nielsen*, *Anja Boisen\**  
22  
23

